

Title

The effect of muscle-tendon unit vs fascicle analyses on vastus lateralis force
generating capacity during constant power output cycling with variable cadence

Abbreviated title

Effects of muscle analysis level on muscle force in cycling

Authors & Affiliations

Scott F Brennan¹, Andrew G Cresswell¹, Dominic J Farris¹, Glen A Lichtwark¹

¹ The University of Queensland, School of Human Movement & Nutrition Sciences,
Centre for Sensorimotor Performance, Brisbane, QLD, Australia, 4072.

Corresponding author

Glen A Lichtwark

The University of Queensland

School of Human Movement & Nutrition Sciences

Brisbane, QLD, Australia, 4072.

E: g.lichtwark@uq.edu.au

P: (+61) 7 3365 3401

Fax: (+61) 7 3365 6877

Keywords

muscle mechanics, muscle tendon unit, fascicle, vastus lateralis

Abstract

The maximum force capacity of a muscle is dependent on the lengths and velocities of its contractile apparatus. Muscle-tendon unit (MTU) length changes can be estimated from joint kinematics, however contractile element length changes are more difficult to predict during dynamic contractions. The aim of this study was to compare vastus lateralis (VL) MTU and fascicle level force-length and force-velocity relationships, and dynamic muscle function while cycling at a constant submaximal power output (2.5 W/kg) with different cadences. We hypothesized that manipulating cadence at a constant power output would not affect VL MTU shortening, but significantly affect VL fascicle shortening. Furthermore, these differences would affect the predicted force capacity of the muscle. Using an isokinetic dynamometer and B-mode ultrasound (US), we determined the force-length and force-velocity properties of the VL MTU and its fascicles. In addition, three-dimensional kinematics and kinetics of the lower limb, as well as US images of VL fascicles were collected during submaximal cycling at cadences of 40, 60, 80 and 100 RPM. Ultrasound measures revealed a significant increase in fascicle shortening as cadence decreased (84% increase across all conditions, $p < 0.01$), whereas there were no significant differences in MTU lengths across any of the cycling conditions (maximum of 6%). The MTU analysis resulted in greater predicted force capacity across all conditions relative to the force-velocity relationship ($p < 0.01$). These results reinforce the need to determine muscle mechanics in terms of separate contractile element and connective tissue length changes during isokinetic contractions as well as dynamic movements like cycling.

51 **New & Noteworthy**

52 We demonstrate that vastus lateralis (VL) muscle tendon unit (MTU) length changes
53 do not adequately reflect the underlying fascicle mechanics during cycling. When
54 examined across different pedaling cadence conditions, the force generating potential
55 measured only at the level of MTU (or joint) overestimated the maximum force capacity
56 of VL compared to analysis using fascicle level data.

Introduction

The characteristic force-length relationship of muscle demonstrates that the greatest force production occurs at a specific length, defined as the optimal fiber length (L_0) (18). At shorter or longer lengths, the maximum capacity of the fiber to produce force is reduced due to a reduction in the effective overlap of its contractile proteins (23, 24). The maximum force producing capacity of muscle fibers is also influenced by the velocity that they shorten or lengthen at during a contraction. At slow shortening velocities, muscles are still capable of producing relatively large forces (22). However, as the velocity of shortening increases, there is an exponential decrease in the maximum force producing capacity of the muscle until reaching its maximum shortening velocity (V_{\max}). The length and velocity properties of muscle therefore constrain the way animals produce force, which subsequently influences their ability to generate the mechanical power that is essential to move the body during cyclical movement tasks such as walking, running and cycling (5).

Estimates of muscle tendon unit (MTU) lengths have been relatively easy to ascertain from kinematic modelling of limb motion. A limitation of using estimates of MTU length changes to infer contractile dynamics of muscle is that this approach does not account for the effects of series elasticity in connective tissues like the aponeuroses and tendons. Recent advances in ultrasound imaging have allowed length changes of the contractile tissue to be measured in human muscle, which now allows for more accurate representations of muscle fascicle length changes and estimates of intrinsic contractile properties. Muscles like the human gastrocnemius and soleus have a long, compliant tendon attached to much shorter muscle fibers (40) giving rise to a large tendon length:muscle fiber length ratio (L_T/L_F) and significant energy recycling within

the tendon during locomotion. Those elastic interactions are particularly important for locomotion, as the stretch and recoil of elastic tissues will affect the muscle's power production and overall efficiency (29). This has been shown in walking and running where the compliance of the series elastic tendon uncouples the length changes of the contractile tissue from the MTU during periods of the gait cycle (28).

While walking and running involve stretch-shortening cycles that enhance muscle and tendon function (25, 30), other repetitive movements like cycling involve primarily concentric work of the lower limb muscles (11). Cycling is particularly interesting in this regard, as it is possible to achieve the same overall power output while utilizing a wide range of gearing and cadence combinations. Maintaining a constant power output at different cadences has little impact on joint range of motion during seated cycling, particularly for the knee (7, 12). The MTU length changes are likely to be similar regardless of cadence because of the constraint that the pedals place on the kinematics. Therefore, MTU velocity should predictably increase with cadence (37). While the MTU length changes are predictable, the muscle forces and activations are less predictable for individual muscles. For instance, there is little change in neuromuscular activity of the vastus medialis or lateralis in response to cadence manipulation for a given power output (38). However, the force-velocity relationship would predict a decrease in force capacity as cadence increases, and therefore an increase in activation to achieve a required submaximal muscle force. It is possible that the discrepancies between shortening velocity, force and activation are linked to the interaction between muscle and tendon and how this influences the length and velocity of the contractile tissue, particularly with different force requirements under varying cadence conditions.

107

108 Even at slow pedal rates (40 RPM) and relatively low power outputs (98 W) there can
109 be discrepancies between the length changes of the muscle fascicles and the
110 associated connective tissues (32). For instance, at low cadences the quadriceps
111 muscles will experience low MTU velocities. However, as the quadriceps contract and
112 force increases they will stretch the series elastic tissue and hence muscle fascicles
113 must shorten at greater velocities than the MTU to increase force output (32).
114 Conversely, as quadriceps force decreases later in the pedal cycle the series elastic
115 tissue will recoil at higher velocity than the fascicles (32). The magnitude of the
116 required forces also affects the stretch of series elastic elements and therefore the
117 operating length of the fascicles. For a given cadence, there is increased fascicle
118 shortening as power output is increased because of the greater force requirements
119 (3), illustrating that fascicle operating length is not only dependent on the knee angle
120 / MTU length, but also on fascicle force. As such, the forces, cadence and the degree
121 of series elastic compliance within the muscle will have a substantial effect on the
122 operating lengths and velocities of the contractile tissue.

123

124 The aim of this study was to explore the operating lengths and velocities of VL at the
125 MTU and fascicle levels during cycling at a constant power output at a range of
126 cadences and to determine how this influences the predicted force generating capacity
127 of the VL muscle. We first characterized the force-length and force-velocity properties
128 of the VL MTU and fascicles using an isokinetic dynamometer and a mono-articular
129 knee extension protocol with synchronous measurement of fascicle length using B-
130 mode ultrasound. We then determined the operating lengths and velocities of the VL
131 MTU and fascicles during cycling relative to those measured using the isokinetic

dynamometer. The MTU level analysis is analogous to basing optimum lengths and velocities on joint kinematics alone, which ignores the potential effect of series elasticity on contractile dynamics. We hypothesized that VL MTU shortening magnitude would not be significantly different across the different cycling cadences, while fascicle analyses would reveal significant differences in length changes across cadences. Furthermore, we predicted that VL MTU velocities would increase linearly with increased cadence due to the greater crank angular velocity, whereas fascicle shortening velocities would not increase with the same magnitude due to the effects of series compliance.

Methods

Eleven participants provided informed consent to participate in the study (age 27 ± 4.5 years, height 178 ± 5.7 cm, mass 73.6 ± 6.8 kg). The study was approved by an institutional ethics committee. Each participant completed two experimental sessions to firstly collect VL force-length and force-velocity data using an isokinetic dynamometer (HUMAC NORM, CSMi Inc., Stoughton, MA, USA), and secondly, using a cycling ergometer (Lode Excaliber Sport, Lode B.V., Groningen, Netherlands) to collect motion data. Fascicle data for one participant was excluded from the analysis because it could not be adequately tracked across all of the trials.

Dynamometer Protocol

A familiarization session was performed 1 to 2 days prior to the experimental data collection to make sure the participants could perform consistent maximal voluntary knee extensor efforts. Participants were seated in the dynamometer with a hip angle of 80° and the dynamometer attachment was adjusted to align with the

rotation axis of the left knee. A 60-s isotonic warm up protocol was then performed using the interactive capacity of the dynamometer, where the participant performs repeated knee extensions to move a cursor within the target pathway presented on screen. The resistance was self-selected; the participant was instructed to select a torque value that corresponded to approximately 50% of their maximal voluntary effort. Subsequently, an isometric protocol was implemented that consisted of randomized blocks of three maximal voluntary isometric efforts from 50{degree sign}-100{degree sign} of knee flexion at 10{degree sign} increments. The isometric angles were selected to include the optimal angle of the torque-angle relationship, and the knee angle range of motion during cycling. A fully extended knee was defined as 0{degree sign}. For each contraction participants were instructed to perform a ramp contraction up to their maximal effort over a 3-s period then hold the maximal effort for 1-s before relaxing. Two minutes of rest was given between efforts to avoid any potential fatigue effects. An isokinetic protocol was then implemented where participants performed randomized blocks of three maximal effort knee extensions from 100{degree sign} flexion to full extension at five angular velocities (50{degree sign}/s, 100{degree sign}/s, 200{degree sign}/s, 300{degree sign}/s, and 400{degree sign}/s). A pre-loading torque was used to reduce the effects of varying activation and series compliance stretch across different isokinetic velocities (26). A torque threshold was set to 90% of the maximum isometric torque at 100{degree sign} to control when the dynamometer began moving (15).

Dynamometer measurements

Knee extensor torque and joint angle were sampled from the analogue output of the dynamometer using a CED Micro 1401 A/D converter (2 kHz) and recorded in Spike

2 software (Cambridge Electronic Design Ltd., Cambridge, England). The torque signal was filtered using a 10 Hz, first-order, low-pass, bi-directional Butterworth filter in Matlab (MathWorks Inc., Natick, MA, USA). Knee extensor torque was gravity corrected using the resting torque at 0{degree sign} (42). Passive torque was calculated as the difference between the resting torque and gravity corrected torque prior to the contraction. The best two-out-of-three trials based on maximal torque were analyzed for each joint angle. For the isokinetic trials, the mean torque and muscle shortening velocity was taken over only the constant angular velocity portion of the movement. This removed any inertial effects on measured torque that would be present during the acceleration periods at the start and end of the movement.

Ultrasound measurements

Measurements of VL fascicles were made using two ultrasound units that enabled the use of two flat ultrasound transducers (LV7.5/60/96Z, TELEMED, Vilnius, Lithuania) that were held end-to-end by a custom made frame. The arrangement enabled the end-to-end visualization of fascicles that could not be similarly seen by either of the transducers individually. A custom Matlab script was written to concatenate the two individual images. A 22 mm gap between the visual fields of the two images occurred as a result of the shape of the transducers, which was accounted for in the concatenation process. The frame was placed at mid-thigh length, following a straight line between the greater trochanter and the superior patella insertion. A self-adhesive compression bandage was used to secure the frame and transducers to the thigh. The central frequency of the transducers was set to 5 MHz, image depth 50 mm, and the sampling rate to 80 Hz. A logic pulse from the first ultrasound unit triggered data capture by the second ultrasound unit, which also produced its own logic pulse. The

two logic pulses were recorded by the A/D board to determine any delay between the onsets of image collection that could be corrected. A semi-automated tracking algorithm was used to measure fascicle length (13, 17). Fascicle lengths were calculated as the distance between the origin of the fascicle in the proximal image and the distal insertion with the deep aponeurosis in the distal image. Markings were made around the location of the ultrasound transducers with a permanent marker so their position could be matched between the dynamometer and cycling sessions.

Dynamometer derived muscle relationships

Quadriceps force was calculated by dividing the measured torque by the angle specific moment arm from each individual scaled musculoskeletal model (9). VL fascicle length was measured from the ultrasound data. VL MTU length was measured as the angle specific MTU lengths from each individual scaled musculoskeletal model. The musculoskeletal model was scaled using measurement-based scaling in OpenSim software, using the anatomical markers placed to collect the kinematic data during cycling.

A fascicle force-length curve and MTU force-length curve was produced for each participant, based on a physiologically appropriate model (4).

$$F_{active} = e^{-|(L^b-1)/s|^a}$$

where F is force, L is length (fascicle or MTU), a is roundness, b is skewness, and s is width of the curve. The curve fit was optimized in Matlab using a nonlinear least squares method. The predicted optimum fascicle length (L_{0_F}) and optimum MTU length (L_{0_MTU}) was constrained to within the range of measured lengths. The b and s coefficients were constrained to a range of 0-4 and 0-2 respectively. The a coefficient

was constrained to a value of 2. These values were selected to achieve force-length curves similar to the characteristic sarcomere force-length relationship (18) and hence ensure that the curve fits were physiological.

A fascicle force-velocity curve and MTU force-velocity curve was also produced for each participant using a physiological model (8) that utilized the optimal length (L_{0_F} or L_{0_MTU}) and isometric force (F_{max}) values from the isometric curve fit data.

$$F = ((1 - (V/V_{max})) \div (1 + (((V/V_{max}) * G)))) \times F_{max}$$

Where V is shortening velocity, V_{max} is the maximum shortening velocity, G is curvature, and F_{max} is the maximum force capacity. For both relationships we allowed a curvature of $3 < G < 9$ and a maximum shortening velocity of $4 < V_{max} < 12 L_0/s$, which are reasonable boundaries based on animal models (10, 27).

The force-length and force-velocity properties for the VL MTU were computed for each individual using the same approach as for the fascicles, however the MTU lengths were used for each joint angle or angular velocity tested. The same curve fitting parameters used in the fascicle analysis were used to construct an MTU force-length relationship for each participant. Fascicle curves were normalized to the predicted L_{0_F} and F_{max} . MTU curves were normalized to the predicted L_{0_MTU} and F_{max} . The force-velocity relationship was constructed by using the mean fascicle or MTU shortening velocity over the isokinetic period. The MTU velocities were normalized to the respective L_{0_MTU} .

Cycling measurements

A six camera motion analysis system (Qualysis, Gothenburg, Sweden) was used to capture, at 200 Hz, the locations of 23 passive, reflective markers positioned on anatomical landmarks on the left thigh, left shank and pelvis. Scaling markers were placed on anatomical landmarks of the anterior and posterior superior iliac spines (left and right), greater trochanter, medial and lateral epicondyles of the femur, medial and lateral malleoli, calcaneus, 1st and 5th metatarsal heads and most distal point of the toes on the left leg. The calcaneus, 1st and 5th metatarsal head, and toe markers were placed on the cycling shoes. Clusters of 4 markers on rigid plates were used for dynamic tracking of the shank and thigh segments. The remaining markers were placed on the iliac crest and sacrum for tracking the pelvis in dynamic movements. The calibration markers on the shoe were used for dynamic tracking of the foot segment. A static calibration capture was recorded as the subject stood with feet shoulder width apart and arms crossed to opposite shoulder. A modified version of the OpenSim gait 2392 model (only pelvis and left limb) was scaled using measurement-based scaling based on the static calibration capture. An inverse kinematics analysis was performed in OpenSim, using a weighted least squares fit between the model markers and experimental markers at each time point. The inverse kinematics analysis was used to measure joint angle, VL MTU length, and subsequently calculate MTU velocity as the time differential of MTU length. Seat height was normalized to 100% trochanter length (6, 33, 34). Participants cycled at a constant power output of 2.5 W/kg body mass, at predetermined cadences of 40 RPM, 60 RPM, 80 RPM and 100 RPM in a randomized order. Shimano SPD-SL pedals and R078 cycling shoes (Shimano Inc., Osaka, Japan) were used for all conditions. Kinematic data was exported for analysis using Matlab and OpenSim. Muscle fascicle length changes

were measured during cycling using the same ultrasound location and technique as the dynamometer section.

Analyses

Statistical analysis was performed in Graphpad Prism 7 (GraphPad Software Inc., La Jolla, CA, USA). The goodness of fit between the measured data points and curve fitting results were measured using R^2 and standard error of the estimate (SEE). The SEE values are reported relative to the individual F_{\max} to demonstrate the error relative to the force-length and force-velocity curves. Curve fit coefficients were compared between MTU and fascicle data using a paired t-test.

Fascicle and MTU lengths were filtered using a 5 Hz, 2nd-order, low-pass, bi-directional Butterworth filter. The magnitude of muscle shortening was calculated as the difference between the maximum and minimum length during the knee extension phase. Muscle shortening velocities were calculated as the time differential of MTU length and fascicle length. Peak shortening velocities during cycling were calculated as the maximum shortening velocity of the MTU and fascicles during the knee extension period. Mean shortening velocities were calculated as the average shortening velocity during the knee extension period. Magnitude of shortening, mean and peak velocity were compared across both analyses level (MTU vs fascicle) and cadence using a two-way repeated measures ANOVA. Multiple comparisons were made across cadences within each level of analysis, with corrections made using the Holm-Sidak test. A one-way repeated measures ANOVA was used to compare the effect of cadence on joint range of motion. The operating lengths represent the MTU and fascicle lengths while the knee is extending (i.e. the push phase of the pedal

cycle). To determine the capacity for force production across conditions, we calculated a *force index* for each participant from their individual force-length and force-velocity relationships, and lengths and velocities recorded across all cycling conditions for the same participant (2). The length-based and velocity-based force index values were equal to the fraction of F_{\max} that could theoretically be produced by a maximally activated muscle at the normalized length or velocity for each time point. For example, if at a single time point the fascicle was active at a length of $1.2 L_0$ it could have a length-based force index of approximately 0.6 (depending on the individual force-length curve). That would mean at that time point the fascicles would have a maximum force capacity of 60% F_{\max} based on length data. The mean force index values were then computed as the average of all the time points during the knee extension period. The same process was applied to the velocity-based force index. The total force index was equal to the length-based force index multiplied by the velocity-based force index and represents the total force generating capacity. The mean force index was compared across level of muscle analysis (MTU vs fascicle) and cadence using a two-way repeated measures ANOVA, with multiple comparisons across cadence. An alpha of 0.05 was set to achieve significance for all tests, with corrections for multiple comparisons. Data shown in text are mean \pm standard deviation.

Results

Dynamometer force vs length relationships

The range of absolute lengths spanned the upper end of the ascending limb, plateau and descending limb of the force-length curve (Figure 1 a,b). The group mean (\pm SD) R^2 values between the measured lengths and predicted curve were 0.84 ± 0.15 for the MTU force-length relationship compared to 0.70 ± 0.16 for the fascicle force-length

relationship. The SEE was equal to 0.04 ± 0.02 for the MTU force-length curve fit and 0.07 ± 0.02 for the fascicle force-length curve fit. The optimal MTU length was observed at 0.26 ± 0.01 m and the optimal fascicle length was 0.11 ± 0.01 m. Normalizing the individual force-length curves to their respective optimal length showed the data was spread across normalized lengths of $0.8 - 1.4 L_0$ (Figure 1 c,d).

Dynamometer force vs velocity relationships

The group mean (\pm SD) R^2 values were 0.82 ± 0.15 for the MTU force-velocity curves and 0.78 ± 0.17 for the fascicle force-velocity curves. The group mean SEE values were 0.09 ± 0.05 for the MTU force-velocity curves and 0.09 ± 0.04 for the fascicle force-velocity curve fits. The isokinetic data showed that the fastest MTU shortening velocities were observed at 45 ± 7 cm/s and fastest fascicle shortening velocities at 13 ± 3 cm/s. This resulted in normalized MTU shortening velocities of approximately $2.0 L_{0_MTU}/s$ for the $400^\circ/s$ joint velocity (Figure 2a). The curvature of the force-velocity fits was significantly different between analysis types ($p = 0.03$). The G coefficient, representing the curvature of the relationship, for the MTU data was 7.39 ± 1.81 compared to 8.85 ± 0.46 for the fascicle data.

Muscle-tendon unit and fascicle length changes during cycling

When analyzing the cycling data, there were significant main effects of muscle analysis and cadence on MTU and fascicle length changes ($p < 0.01$). The knee joint ROM was not significantly different across the range of cadences ($79.0 \pm 6.3^\circ$ at 40 RPM, $76.3 \pm 4.0^\circ$ at 100 RPM), which resulted in similar MTU length changes across cadences ($0.21 L_{0_MTU} \pm 0.06$, $p = 0.07$). Fascicle length changes significantly decreased with increasing cadence ($p < 0.01$), from 0.31 ± 0.07

L_{0_F} at 40 RPM to $0.16 \pm 0.05 L_{0_F}$ at 100 RPM. There was also a significant interaction between factors ($p < 0.01$), further illustrating that length changes across cadences did not show the same pattern for both the MTU and fascicle analysis.

VL MTU and fascicle lengths, over a crank cycle, were plotted against the respective VL force-length curves to determine their operating range. The VL MTU lengths covered the optimum of the force-MTU length curve (Figure 3a), operating across the same range for all cadences ($0.90 \pm 0.02 - 1.07 \pm 0.02 L_{0_MTU}$, $p = 0.10$). VL fascicles started each cycle at similar relative operating lengths ($1.2 \pm 0.02 L_{0_F}$) on the descending limb of the force-length curve for all cadences, and shortened by greater relative magnitudes at slower cadences compared to faster cadences (Figure 3b).

There was a significant effect of cadence and analysis on peak shortening velocity ($p < 0.01$), with a significant interaction between cadence and analysis ($p < 0.01$). The peak MTU shortening velocity predictably increased with cadence by 50%, 99% and 144% as cadence increased from 40 to 60, 80 and 100 RPM respectively (Table 1). The peak fascicle shortening velocity increased with cadence by 28%, 46% and 52% respectively as cadence increased from 40 to 60, 80 and 100 RPM. The absolute fascicle shortening velocities were faster than the absolute MTU shortening velocities during the early pedal cycle across all cadence conditions (Figure 4). For the 40 and 60 RPM conditions, there was both a higher peak fascicle velocity and an earlier occurrence of peak shortening velocity compared to the MTU (Table 1). For the 80 and 100 RPM conditions the peak absolute MTU velocity was higher, but the occurrence of peak fascicle shortening velocity was approximately 15% earlier in the pedal cycle. There was also significant effects of cadence and analysis level on mean

fascicle shortening velocity ($p < 0.01$) with a significant interaction between factors ($p < 0.01$). The multiple comparisons test showed the mean MTU shortening velocity significantly increased between all cadence conditions ($p < 0.01$). However, the average fascicle shortening velocity plateaued between the 80 RPM and 100 RPM conditions (8.6 ± 2.7 and 8.5 ± 2.1 cm/s). For both the MTU and the fascicle analyses there was a clear pattern for higher peak relative shortening velocities as cadence increased (Figure 5, $p < 0.01$).

The group mean force indices during the knee extension phase showed that shortening velocity had a greater influence on the capacity for force production compared to the operating length for both the MTU and fascicle data. The mean length-based force index (force-length index) was not significantly affected by the analysis type ($p = 0.68$) or cadence ($p = 0.07$), maintaining a mean value across conditions of 75% and 78% maximum force capacity for the MTU and fascicles respectively (Figure 6a). The mean velocity-based force index (force-velocity index) was significantly affected by both analysis method and cadence ($p < 0.01$) with a significant interaction effect ($p = 0.01$). The MTU force-velocity index was overall higher and decreased consistently with increased cadence. The fascicle force-velocity index decreased with increasing velocity, however the slope of this relationship was reduced with increasing velocity and plateaued between 80 RPM and 100 RPM (Figure 6b). The mean force index based on length and velocity (total force index) was significantly affected by both analysis and cadence ($p < 0.01$) with no significant interaction effect ($p = 0.42$).

Discussion

This study investigated the effect of analyzing the length changes of the VL MTU versus VL fascicles on the predicted force potential while cycling with a constant power output and different cadences. The force index values represented the capacity for force production during cycling relative to that which could theoretically be produced by a maximally activated muscle at the normalized length or velocity. The results showed that considering only the MTU length changes to predict force generating capacity, and ignoring the effect of series elastic contributions, does not adequately reflect how the contractile dynamics change with increasing cadence. The MTU analysis resulted in consistent length changes across cadence conditions because of the kinematic constraints, whereas the fascicle analysis was able to detect the force-related differences in shortening as cadence was manipulated. MTU shortening velocity increased progressively with cadence, whereas the fascicle velocity did not increase at higher cadences and therefore the VL muscle likely maintained force generating capacity at higher cadences. As such, using a joint kinematics or MTU length measurement to predict muscle performance across different cycling conditions is unlikely to yield valid information about optimal cycling technique or posture.

Muscle-tendon unit and fascicle length changes during cycling

The interaction between muscle fibers and series elastic tissues are important when applied to dynamic movements like cycling. During cycling, the overall movement pattern remains relatively constant in relation to the crank position, while the muscle forces and velocities vary with different gearing and cadence combinations. The constraints of the bicycle resulted in predictable MTU length changes because the knee joint angular displacement is relatively unaffected by cadence. Thus, we did not

observe significant changes in MTU shortening across cadence conditions, and it resulted in consistent force-length index values. However, the elasticity of the tendon may augment the length changes of the fascicles to different degrees depending on the force requirements dictated by maintaining a constant power output across different cadences. The amount of fascicle shortening was affected by cadence (unlike the MTU shortening), with greater fascicle shortening at low cadences because of the increased force requirements and corresponding strain on the series elastic tissues. Despite the increased fascicle shortening at low cadences, the greater range of operating lengths did not reduce the fascicle force-length index. While these effects did not translate to a significant difference in the capacity for force production, based on the force-length index, they may be important in terms of separating fascicle and tendon work throughout the pedal cycle.

The consistent decrease in the MTU force-velocity index as cadence increased was not observed for the fascicles. The slope of the relationship between fascicle force-velocity index and cadence reduced with increasing cadence and plateaued at the highest cadences (80-100RPM). At low cadences the pedal forces are greater, which imposes a greater strain on the series elastic tissues. Early in the pedal cycle, while quadriceps force is rising, the absolute fascicle shortening velocity exceeds the absolute MTU shortening velocity in order to stretch the tendon before it recoils during force decline (32). At 40 RPM the peak fascicle shortening velocity is greater than the peak MTU shortening velocity and occurs approximately 5% earlier in the pedal cycle (Table 1). As cadence increased, the required pedal forces are reduced to maintain constant power. The lower forces and higher velocity resulted in a disproportionate increase in peak MTU shortening velocity compared to the fascicles (144% vs 52% from 40 – 100 RPM), and a much earlier occurrence of peak fascicle shortening

velocity compared to the MTU, which maintained consistent timing relative to the pedal cycle. The MTU analysis does not detect the force related differences in absolute shortening velocity of the fascicles and series elastic tissues while cycling at different cadences (Figure 4, Table 1). These findings show that an MTU analysis results in a higher predicted maximum force generating capacity during cycling, because the MTU velocities during cycling (even at 100 RPM) are low relative to the maximal shortening velocity of the muscle (20). However, the MTU analysis also predicted a decrease in force generating capacity across the range of cadences tested, whereas this relationship was non-linear when considering fascicle dynamics. Fascicle level analyses showed that force generating capacity plateaued at higher cadences and this can be explained by the high velocity shortening late in the pedal cycle being performed by the series elastic tissue.

Dynamometer measurements for predicting force generating capacity

The interaction between muscle fibers and tendon can affect the mechanical performance of the muscle during contractions, and therefore influence predictions of muscle force capacity (19, 31). Despite the constant angular velocity of the movement, the force capacity of the muscle is crucially dependent on the length changes of the fascicles because they represent the contractile apparatus. The fascicle shortening velocity can be slower or faster than the MTU depending on the forces produced (15, 20). These force dependent length changes between contractile tissue and elastic tissue impact our predictions of muscle force capacity if there is not an appropriate differentiation between the two tissues. We have measured similar fascicle velocities across the range of joint angular velocities investigated compared to similar isokinetic and isotonic studies (15, 20). However, due to the contribution of the series elastic

tissue to overall shortening during high velocities (e.g. quick-release experiments – Hauraix et al. 2017), it is unlikely that our data would be able to predict maximum shortening velocities for the MTU. In this study, the MTU data was normalized to the optimal MTU length rather than traditionally normalizing to L_{0_F} . This would have the effect of reducing the magnitude of the relative velocities, but does not influence the trends in shortening velocity across conditions.

In addition, the use of a pre-activation in our protocol may influence the prediction of MTU force-generating capacity. It has been reported that the force-velocity relationship measured using dynamometry is sensitive to the activation of the muscle (26) and hence undertaking isokinetic tests with no pre-activation could result in different F-V curves, particularly at higher speeds where activation levels may vary (20). However, having a pre-activation should provide us with an estimate of the maximum force producing capacity of the muscle when close to maximum activation.

Limitations

Knee extensor torque was measured as an indication of the VL force during isometric and isokinetic contractions. While approximations of force generation from the VL can be made based on the relative volume of the VL (1), there are changes in the relative activation of the different quadriceps muscles throughout the knee joint range of motion (36, 41), which may influence force estimations. In addition, three dimensional muscle deformation may affect measurement of quadriceps fascicle lengths, which has been shown in the gastrocnemius (21) and tibialis anterior (35). Fascicles and aponeuroses were assumed to be straight lines to estimate fascicle length, which has been found to result in a 2-7% underestimation when using a single transducer method

(14). However, the dual-transducer method used here should have reduced the underestimation error in tracking the distal insertion of the fascicle, and it is less likely to affect fascicle shortening velocities in the repeated measures design used in this study. Finally, we did not examine the full range of isometric joint angles or very high joint angular velocities (16, 20, 39), which means the prediction of the isometric force capacity and maximal shortening velocity may be improved by measurement of data approaching these extremities. However, the range of joint angles and velocities examined here was within the range experienced during the relevant cycling conditions (eg. 100 RPM equals approximately 400 {degree sign}/s). Our estimates of force generating capacity should be consistent within the range tested, while our estimates of V_{\max} may be susceptible to errors in curve fitting across the more narrow velocity range; particularly if the series elastic tissue contribution increases at greater MTU shortening velocities.

Conclusions

Analyzing muscle mechanics at a MTU level (or joint level) versus fascicle level can have significant implications for interpretations of muscle mechanics during cycling. Changes in force with cadence influence the instantaneous velocities of the fascicles in relation to the MTU. The fascicles may be shortening faster, similarly, or at a slower velocity than the MTU, depending on the instantaneous kinematic and force requirements. Our results showed that the estimated force capacity of the VL relative to the force-length relationship was not significantly affected by the type of muscle analysis used. However, the estimated force capacity relative to the force-velocity relationship was lower for fascicles compared to the MTU analysis, and in contrast to the MTU analysis, did not consistently decrease as cadence increased (especially at

higher cadences). Thus, examining either MTU length changes or joint kinematics will not provide a good indication of the force generating capacity of muscle across cadence and gearing conditions. The results emphasized that either joint position or MTU length measures may not be very useful to determine the conditions which may maximize muscle force generating capacity during the cycling movement, particularly at higher cadences. Further examination into how changes in power or cycling posture (e.g. seat height) might influence force generating capacity are also warranted.

Acknowledgements

The authors would like to thank the participants for their time and effort.

Grants

Scott Brennan was supported by an Australian Postgraduate Award scholarship.

Disclosures

The authors have no financial or intellectual conflict of interest to declare.

References

1. **Akima H, Kuno S-Y, Fukunaga T, Katsuta S.** Architectural properties and specific tension of human knee extensor and flexor muscles based on magnetic resonance imaging. *Jpn J Phys Fit Sport* 44: 267–278, 1995.
2. **Arnold EM, Hamner SR, Seth A, Millard M, Delp SL.** How muscle fiber lengths and velocities affect muscle force generation as humans walk and run at different speeds. *J Exp Biol* 216: 2150–2160, 2013.
3. **Austin N, Nilwik R, Herzog W.** In vivo operational fascicle lengths of vastus lateralis during sub-maximal and maximal cycling. *J Biomech* 43: 2394–2399, 2010.
4. **Azizi E, Roberts TJ.** Muscle performance during frog jumping: influence of elasticity on muscle operating lengths. *Proc R Soc B* 277: 1523–1530, 2010.
5. **Biewener AA.** Locomotion as an emergent property of muscle contractile dynamics. *J Exp Biol* 219: 285–294, 2016.
6. **Bini RR, Hume PA, Crofta JL.** Effects of saddle height on pedal force effectiveness. *Procedia Engineering* 13: 51–55, 2011.
7. **Bini RR, Tamborindéguy AC, Mota CB.** Effects of saddle height, pedaling cadence, and workload on joint kinetics and kinematics during cycling. *J Sport Rehabil* 19: 301–314, 2010.
8. **Curtin NA, Woledge RC.** Power output and force-velocity relationship of live fibres from white myotomal muscle of the dogfish, *Scylliorhinus Canicula*. *J Exp Biol* 140: 187–197, 1988.

- 572 9. **Delp SL, Loan JP, Hoy MG, Zajac FE, Topp EL, Rosen JM.** An interactive
573 graphics-based model of the lower extremity to study orthopaedic surgical
574 procedures. *IEEE Trans Biomed Eng* 37: 757–767, 1990.
- 575 10. **Edman KA, Mulieri LA, Scubon-Mulieri B.** Non-hyperbolic force-velocity
576 relationship in single muscle fibres. *Acta Physiol Scand* 98: 143–156, 1976.
- 577 11. **Ericson MO, Bratt Å, Nisell R, Arborelius UP, Ekholm J.** Power output and
578 work in different muscle groups during ergometer cycling. *Eur J Appl Physiol* 55:
579 229–235, 1986.
- 580 12. **Ericson MO, Nisell R, Németh G.** Joint Motions of the Lower Limb during
581 Ergometer Cycling. *J Orthop Sports Phys Ther* 9: 273–278, 1988.
- 582 13. **Farris DJ, Lichtwark GA.** UltraTrack: Software for semi-automated tracking of
583 muscle fascicles in sequences of B-mode ultrasound images. *Comput Methods*
584 *Programs Biomed* 128: 111–118, 2016.
- 585 14. **Finni T, Ikegawa S, Lepola V, Komi PV.** Comparison of force-velocity
586 relationships of vastus lateralis muscle in isokinetic and in stretch-shortening cycle
587 exercises. *Acta Physiol Scand* 177: 483–491, 2003.
- 588 15. **Fontana H de B, Roesler H, Herzog W.** In vivo vastus lateralis force-velocity
589 relationship at the fascicle and muscle tendon unit level. *J Electromyogr Kinesiol*
590 24: 934–940, 2014.
- 591 16. **Forrester SE, Yeadon MR, King MA, Pain MTG.** Comparing different
592 approaches for determining joint torque parameters from isovelocity dynamometer
593 measurements. *J Biomech* 44: 955–961, 2011.

- 594 17. **Gillett JG, Barrett RS, Lichtwark GA.** Reliability and accuracy of an automated
595 tracking algorithm to measure controlled passive and active muscle fascicle length
596 changes from ultrasound. *Comput Methods Biomech Biomed Eng* 16: 678–687,
597 2013.
- 598 18. **Gordon AM, Huxley AF, Julian FJ.** The variation in isometric tension with
599 sarcomere length in vertebrate muscle fibres. *J Physiol-London* 184: 170–192,
600 1966.
- 601 19. **Griffiths RI.** Shortening of muscle fibres during stretch of the active cat medial
602 gastrocnemius muscle: the role of tendon compliance. *J Physiol-London* 436:
603 219–236, 1991.
- 604 20. **Hauraix H, Dorel S, Rabita G, Guilhem G, Nordez A.** Muscle fascicle shortening
605 behaviour of vastus lateralis during a maximal force-velocity test. *Eur J Appl*
606 *Physiol* 117: 289–299, 2017.
- 607 21. **Herbert RD, Héroux ME, Diong J, Bilston LE, Gandevia SC, Lichtwark GA.**
608 Changes in the length and three-dimensional orientation of muscle fascicles and
609 aponeuroses with passive length changes in human gastrocnemius muscles. *J*
610 *Physiology* 593: 441–455, 2015.
- 611 22. **Hill AV.** The heat of shortening and the dynamic constants of muscle. *P Roy Soc*
612 *B-Biol Sci* 126: 136–195, 1938.
- 613 23. **Huxley AF, Simmons RM.** Proposed Mechanism of Force Generation in Striated
614 Muscle. *Nature* 233: 533–538, 1971.
- 615 24. **Huxley H, Hanson J.** Changes in the cross-striations of muscle during contraction

and stretch and their structural interpretation. *Nature* 173: 973–976, 1954.

25. **Ishikawa M, Pakaslahti J, Komi PV.** Medial gastrocnemius muscle behavior during human running and walking. *Gait Posture* 25: 380–384, 2007.

26. **Jensen RC, Warren B, Laursen C, Morrissey MC.** Static pre-load effect on knee extensor isokinetic concentric and eccentric performance. *Med Sci Sports Exerc* 23: 10–14, 1991.

27. **Julian FJ, Rome LC, Stephenson DG, Striz S.** The maximum speed of shortening in living and skinned frog muscle fibres. *J Physiol-London* 370: 181–199, 1986.

28. **Lichtwark GA, Bougoulas K, Wilson AM.** Muscle fascicle and series elastic element length changes along the length of the human gastrocnemius during walking and running. *J Biomech* 40: 157–164, 2007.

29. **Lichtwark GA, Wilson AM.** Effects of series elasticity and activation conditions on muscle power output and efficiency. *J Exp Biol* 208: 2845–2853, 2005.

30. **Lichtwark GA, Wilson AM.** Interactions between the human gastrocnemius muscle and the Achilles tendon during incline, level and decline locomotion. *J Exp Biol* 209: 4379–4388, 2006.

31. **Lieber RL, Brown CG, Trestik CL.** Model of muscle-tendon interaction during frog semitendinosus fixed-end contractions. *J Biomech* 25: 421–428, 1992.

32. **Muraoka T, Kawakami Y, Tachi M, Fukunaga T.** Muscle fiber and tendon length changes in the human vastus lateralis during slow pedaling. *J Appl Physiol* 91: 2035–2040, 2001.

- 638 33. **Nordeen-Snyder KS**. The effect of bicycle seat height variation upon oxygen
639 consumption and lower limb kinematics. *Med Sci Sports* 9: 113–117, 1976.
- 640 34. **Peveler WW**. Effects of Saddle Height on Economy in Cycling. *J Strength Cond*
641 *Res* 22: 1355–1359, 2008.
- 642 35. **Raiteri BJ, Cresswell AG, Lichtwark GA**. Three-dimensional geometrical
643 changes of the human tibialis anterior muscle and its central aponeurosis
644 measured with three-dimensional ultrasound during isometric contractions. *PeerJ*
645 4: e2260, 2016.
- 646 36. **Saito A, Akima H**. Knee joint angle affects EMG-force relationship in the vastus
647 intermedius muscle. *J Electromyogr Kinesiol* 23: 1406–1412, 2013.
- 648 37. **Sanderson DJ, Martin PE, Honeyman G, Keefer J**. Gastrocnemius and soleus
649 muscle length, velocity, and EMG responses to changes in pedalling cadence. *J*
650 *Electromyogr Kinesiol* 16: 642–649, 2006.
- 651 38. **Sarre G, Lepers R, Maffiuletti N, Millet G, Martin A**. Influence of cycling cadence
652 on neuromuscular activity of the knee extensors in humans. *Eur J Appl Physiol*
653 88: 476–479, 2003.
- 654 39. **Thorstensson A, Grimby G, Karlsson J**. Force-velocity relations and fiber
655 composition in human knee extensor muscles. *J Appl Physiol* 40: 12–16, 1976.
- 656 40. **Trestik CL, Lieber RL**. Relationship between Achilles tendon mechanical
657 properties and gastrocnemius muscle function. *J Biomech Eng* 115: 225–230,
658 1993.
- 659 41. **Westing SH, Cresswell AG, Thorstensson A**. Muscle activation during maximal

660 voluntary eccentric and concentric knee extension. *Eur J Appl Physiol* 62: 104–
661 108, 1991.

662 42. **Westing SH, Seger JY.** Eccentric and Concentric Torque-Velocity
663 Characteristics, Torque Output Comparisons, and Gravity Effect Torque
664 Corrections for the Quadriceps and Hamstring Muscles in Females. *Int J Sports*
665 *Med* 10: 175–180, 1989.

666

667

Figure legends

Figure 1. Absolute and normalized force-length curves at the MTU and fascicle level. The absolute MTU lengths (a) and fascicle lengths (b) were consistent with the reported L_0 values in the literature. Horizontal axis represents the absolute (a, b) VL muscle tendon unit (MTU) and VL fascicle length, and (c, d) normalized to the individual optimal lengths (L_{0_MTU} and L_{0_F}). Vertical axis shows the absolute quadriceps force (a, b) and (c, d) normalized to the predicted maximal force (F_{max}). Each cross represents an individual data point for each trial, across all participants.

Figure 2. Individual force-velocity curves for the isokinetic measurements. The decrease in force as shortening velocity increased was less pronounced for the VL muscle tendon unit (MTU) data (a) compared to the VL fascicle data (b). Each cross represents an individual data point for each trial, for all participants. Data points are normalized to the corresponding individual's maximum force (F_{max}) and optimal length (L_{0_MTU} or L_{0_F}). The horizontal axis has been cropped to a maximum of $3.0 L_0/s$ for clarity.

Figure 3. Vastus lateralis (VL) muscle tendon unit (MTU) and fascicle length changes during cycling. The operating lengths of the MTU (a) and fascicles (b) are plotted against the respective group mean force-length curves. The muscle begins actively shortening just prior to top-dead-center (TDC), extending the knee until approximately 45% of the pedal cycle, then relaxing near bottom-dead-centre (BDC) and passively lengthening to return to the upper operating length. (a) The range of operating lengths spanned the plateau region of the MTU data, without a consistent trend across cadence conditions. (b) The fascicle data started at longer normalized lengths and

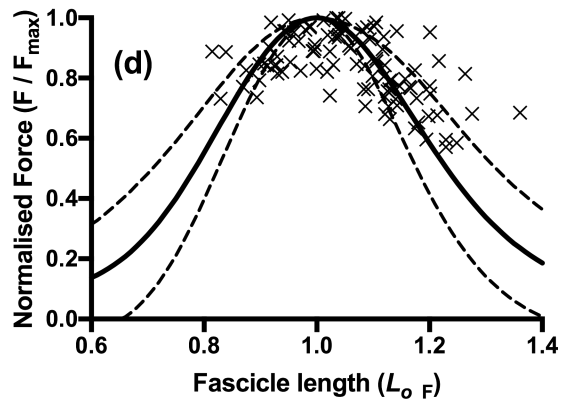
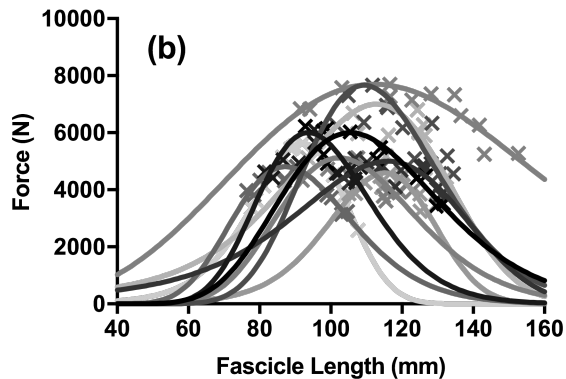
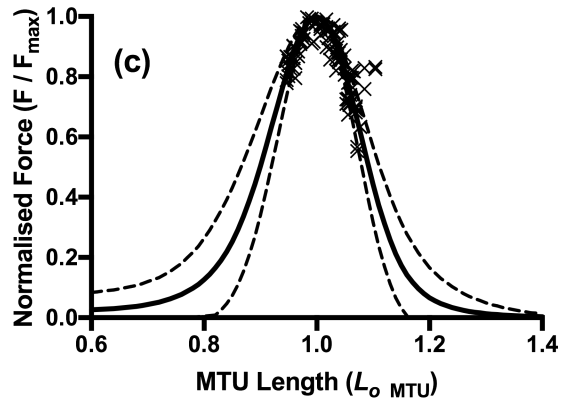
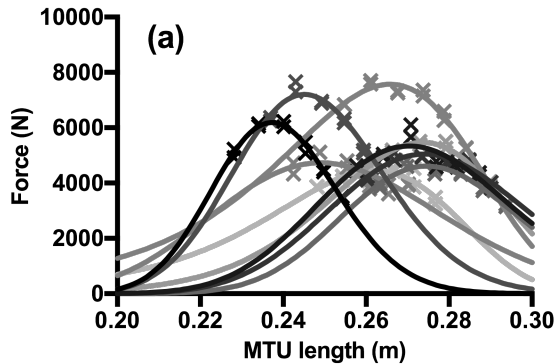
shortened by a significantly smaller magnitude as cadence increased. The vertical lines represent the upper and lower limits of the MTU and fascicle operating lengths for each cadence condition. The circular arrows represent the pattern of length changes as the muscle shortens (TDC-BDC, large arrow) and passively lengthens (BDC-TDC, small arrow). Shaded regions represent -1 SE below the minimum and +1 SE above the maximum of the 40 RPM and 100 RPM conditions to demonstrate variability.

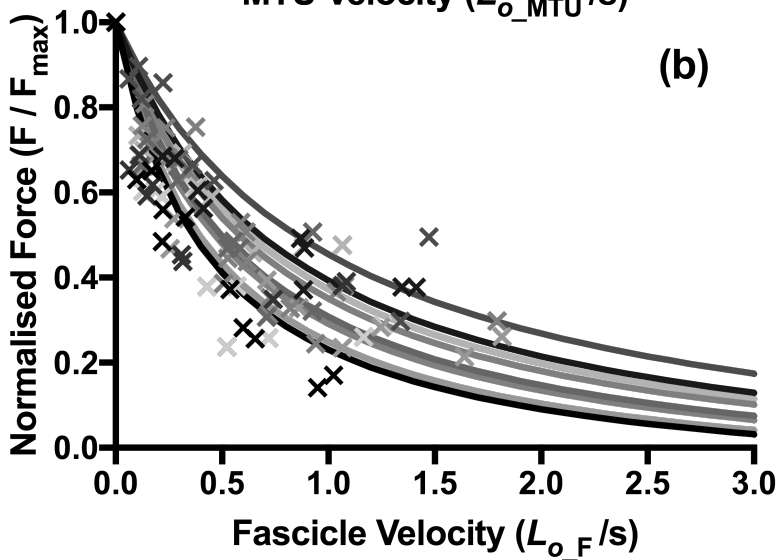
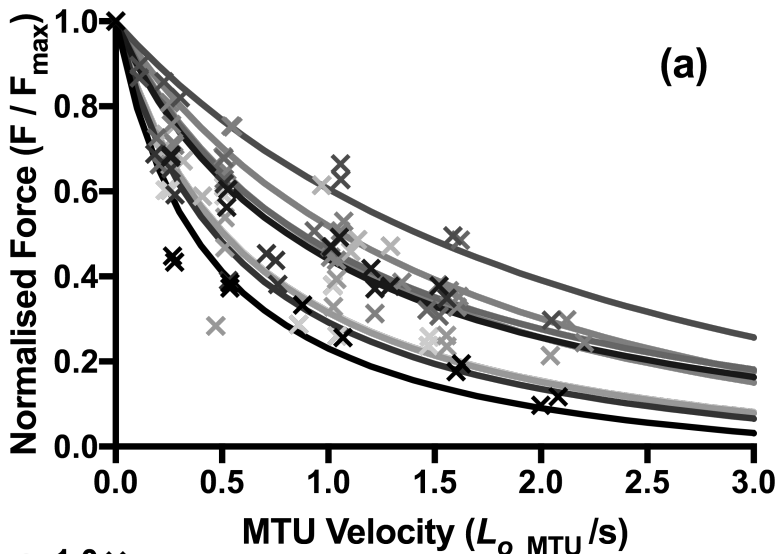
Figure 4. Group mean MTU and fascicle shortening velocity waveforms across cadence. The magnitude of (a) MTU shortening velocity predictably increased as cadence increased whereas (b) the fascicle shortening velocity appeared to plateau at high cadence. The red lines represent the start and stop of the knee extension phase (approximately 95% - 45% of the pedal cycle). The shaded area represents the knee flexion phase that was not included in the analysis. The vertical axis represents muscle velocity normalised to the respective (a) MTU and (b) fascicle L_0 values. The horizontal axis is expressed as a time normalized percentage of the pedal cycle from the vertical crank position.

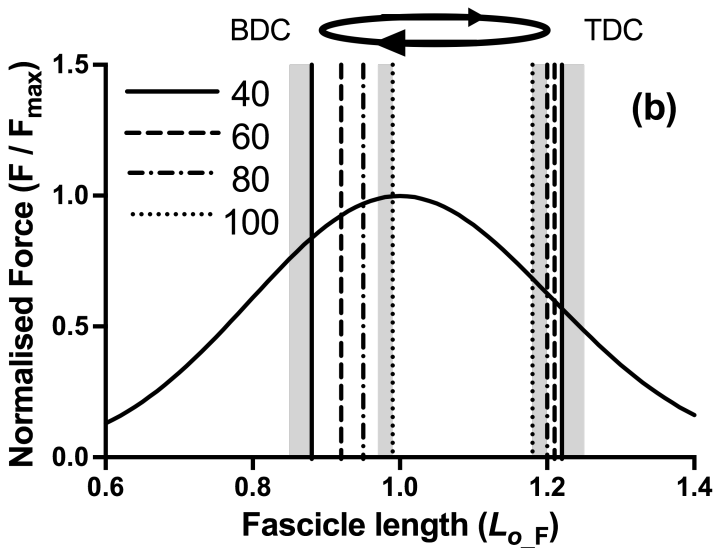
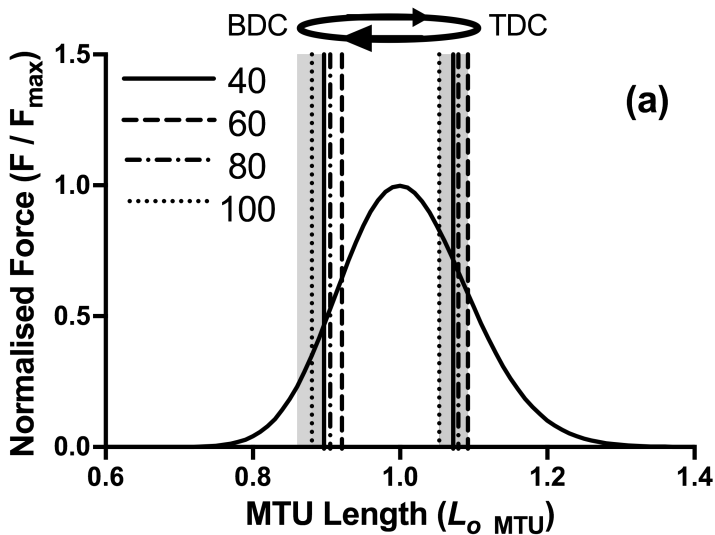
Figure 5. Range of vastus lateralis (VL) muscle tendon unit (MTU) and fascicle shortening velocities (relative to optimum) during cycling. The peak velocities of the (a) MTU and (b) fascicles are plotted against the respective group mean force-velocity curve. The range of shortening velocities across cadences was lower for the MTU relative to the compared to the fascicle shortening velocity (b). At the start of the push phase the VL fascicles and MTU are close to isometric and start to shorten immediately prior to top-dead-center (TDC). The vertical lines show the mean peak

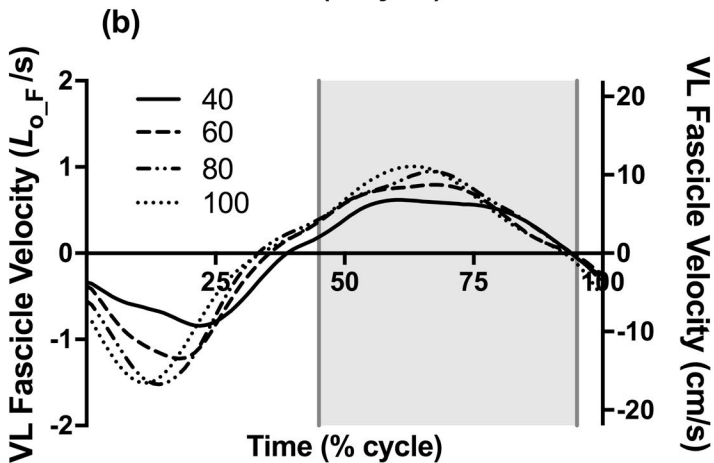
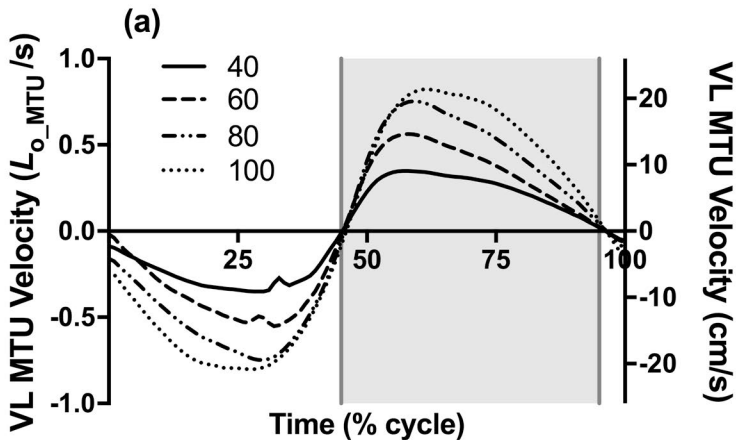
shortening velocities for each of the four cycling cadences. Shaded areas represent ± 1 SE of the 40 RPM and 100 RPM conditions. Error markings are omitted for the 60 RPM and 80 RPM conditions for clarity.

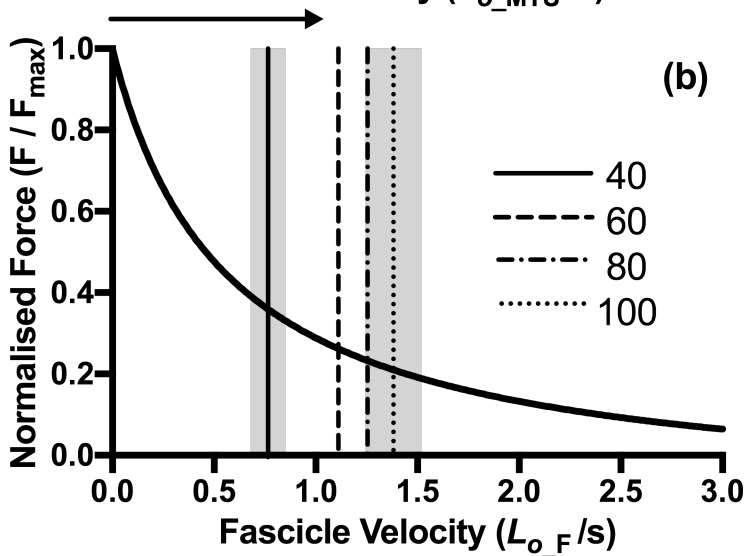
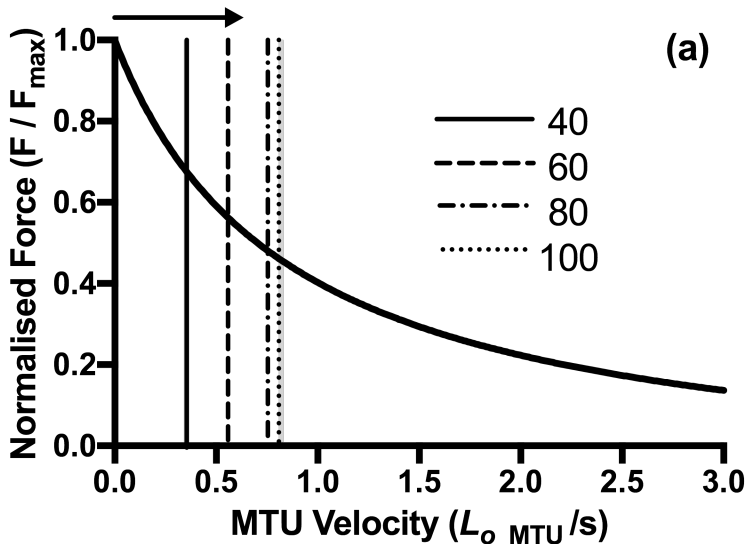
Figure 6. Mean force indices for the vastus lateralis muscle tendon unit (MTU) and fascicle analysis methods relative to cadence. There was no significant difference in the force-length index (a) values between analyses or cadences. The force-velocity index (b) at the MTU decreased linearly with increased cadence, and was always greater than the force index of the fascicles. The total force index was greater in the MTU analysis than fascicle analysis, with a linear decrease as cadence increased. Data shown are mean \pm SD. Data are offset relative to cadence for clarity between overlapping points and error bars.











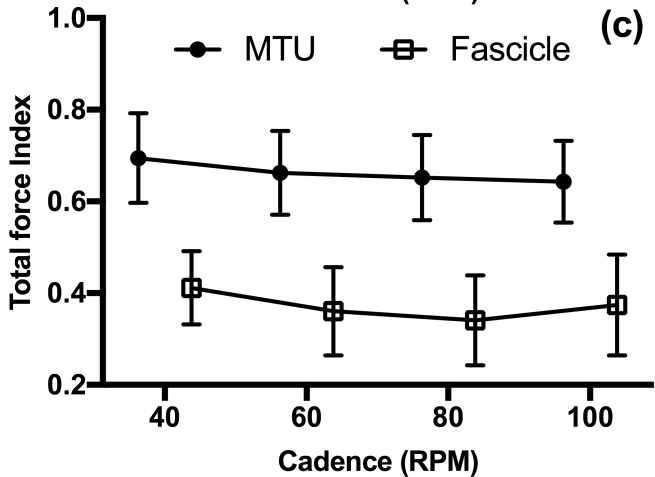
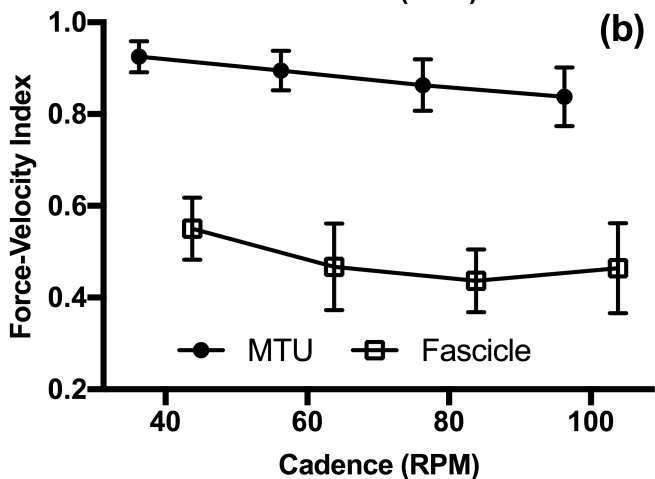
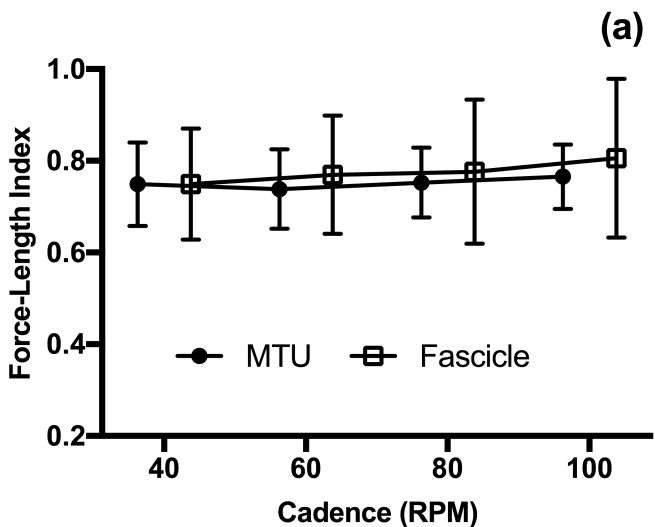


Table 1. Mean and peak absolute shortening velocities of the MTU and fascicles during cycling.

Cadence	MTU		Fascicle	
	mean shortening velocity	peak shortening velocity	mean shortening velocity	peak shortening velocity
40	6.6 ± 0.7	10.1 ± 1.1 (31 ± 4)	5.2 ± 0.9	12.0 ± 2.7 (25 ± 5)
60	9.4 ± 1.3	15.2 ± 1.6 (32 ± 3)	7.6 ± 1.7	15.3 ± 3.6 (18 ± 4)
80	13.3 ± 1.2	20.1 ± 2.1 (30 ± 2)	8.6 ± 2.7	17.5 ± 4.9 (15 ± 4)
100	16.0 ± 2.4	24.6 ± 2.5 (30 ± 4)	8.5 ± 2.1	18.2 ± 5.3 (14 ± 6)

Values for the MTU and fascicles are shown as mean ± SD in cm/s. Values in brackets represent the occurrence of peak velocity as a percentage of the pedal cycle (mean ± SD). There was a significant main effect of cadence and analysis level on mean and peak shortening velocity of both the MTU and fascicles ($p < 0.01$) with a significant interaction. All cadence conditions were significantly different for both the mean and peak MTU shortening velocity. The mean fascicle shortening velocity at 40 RPM was significantly different to the 60, 80 and 100 RPM conditions. The peak fascicle shortening velocity at 40 RPM was significantly different to 100 RPM.